Articles

The K15 Protein of Kaposi's Sarcoma-Associated Herpesvirus Recruits the Endocytic Regulator Intersectin 2 through a Selective SH3 Domain Interaction†

Caesar S. Lim,‡,§ Bruce T. Seet,§ Robert J. Ingham,|| Gerald Gish,‡ Liudmila Matskova,⊥ Gösta Winberg,⊥ Ingemar Ernberg,⊥ and Tony Pawson*,‡,§

Samuel Lunenfeld Research Institute, Mount Sinai Hospital, Toronto, Ontario M5G 1X5, Canada, Department of Biology and Centre for Biomedical Research, University of Victoria, Victoria, British Columbia V8W 3N5, Canada, Karolinska Institutet, Microbiology and Tumor Biology Center (MTC), SE-171 77 Stockholm, Sweden, and Department of Molecular and Medical Genetics, University of Toronto, Toronto, Ontario M5S 1A8, Canada

Received February 20, 2007; Revised Manuscript Received June 11, 2007

ABSTRACT: Kaposi's sarcoma-associated herpesvirus, also known as human herpesvirus 8, is closely associated with several cancers including Kaposi's sarcoma, primary effusion lymphoma, and multicentric Castleman's disease. The rightmost end of the KSHV genome encodes a protein, K15, with multiple membrane-spanning segments and an intracellular carboxy-terminal tail that contains several conserved motifs with the potential to recruit interaction domains (i.e., SH2, SH3, TRAF) of host cell proteins. K15 has been implicated in downregulating B cell receptor (BCR) signaling through its conserved motifs and may thereby play a role in maintaining viral latency and/or preventing apoptosis of the infected B cells. However, K15's mode of action is largely unknown. We have used mass spectrometry, domain and peptide arrays, and surface plasmon resonance to identify binding partners for a conserved proline-rich sequence (PPLP) in the K15 cytoplasmic tail. We show that the PPLP motif selectively binds the SH3-C domain of an endocytic adaptor protein, Intersectin 2 (ITSN2). This interaction can be observed both in vitro and in cells, where K15 and ITSN2 colocalize to discrete compartments within the B cell. The ability of K15 to associate with ITSN2 suggests a new role for the K15 viral protein in intracellular protein trafficking.

Kaposi's sarcoma- (KS-)[1] associated herpesvirus (KSHV), also known as human herpesvirus 8, is a γ2-herpesvirus that is the causative agent of KS and is associated with a number of other lymphoproliferative diseases (*1*). KSHV was first discovered in 1994 by Chang et al. in KS tissue from a patient with AIDS (*2*); however, it is also associated with all forms of KS including classical, endemic, AIDS-associated, and iatrogenically acquired KS (*3*). Since then, KSHV has been shown to infect primarily endothelial cells, as well as B cells, where it is associated with two types of B cell lymphomas including multicentric Castleman's disease (MCD) and primary effusion lymphoma (PEL) (*4*−*6*). A number of genes unique to the KSHV genome are thought to be responsible for KS pathogenesis, one of which is the K15 gene found at the rightmost end of the viral genome (*7*).

The K15 protein of KSHV spans the membrane multiple times, with up to 12 predicted transmembrane sequences, and has intracellular amino- (N-) and carboxy- (C-) terminal tails. In addition to several splice variants which result in differing numbers of transmembrane elements, two different K15 amino acid sequences have been identified and termed the predominant (P) and minor (M) alleles, which possess roughly 33% amino acid sequence identity (*8*, *9*). Interestingly, the C-terminal cytoplasmic regions of the P and M alleles share several short peptide motifs that could recruit signaling molecules. These sites include a putative Src homology 3 (SH3) domain-binding motif, a tyrosine phosphorylation site with the potential to serve as an SH2 domain-binding motif, a putative TRAF-binding motif, and a conserved motif with the amino acid sequence YASIL (*8*, *10*).

† This work was supported by grants from the Canadian Institutes for Health Research (CIHR) and Genome Canada to T.P. and from the Swedish Cancer Society, Grant K2007-68X-20474-01-3, to I.E. T.P. is a Distinguished Investigator of the CIHR. B.T.S. was supported by a postdoctoral fellowship from the Cancer Research Institute (New York).

* To whom correspondence should be addressed at Mount Sinai Hospital. Phone: 416-586-4800 ext 4524. Fax: 416-586-8869. E-mail: pawson@mshri.on.ca.

‡ Mount Sinai Hospital, Toronto.

§ University of Toronto.

|| University of Victoria, Victoria.

⊥ Karolinska Institutet.

[1] Abbreviations: KS, Kaposi's sarcoma; KSHV, Kaposi's sarcoma-associated herpesvirus; MCD, multicentric Castleman's disease; PEL, primary effusion lymphoma; SH3/SH2, Src homology 3/2; pTyr, phosphotyrosine; LMP2A, latent membrane protein 2A; EBV, Epstein−Barr virus; BCR, B cell receptor; mAb, monoclonal antibody; pAb, polyclonal antibody; HRP, horseradish peroxidase; FCS, fetal calf serum; PEI, poly(ethylenimine); BSA, bovine serum albumin; PBS, phosphate-buffered saline; TBST, Tris-buffered saline containing 0.05% Tween 20; ECL, enhanced chemiluminescence; SDS−PAGE, sodium dodecyl sulfate−polyacrylamide gel electrophoresis; LC-MS/MS, liquid chromatography−tandem mass spectrometry; SPR, surface plasmon resonance; Ig, immunoglobulin; Eps15R, Epsin15-related protein; ITSN2, Intersectin 2.

10.1021/bi700357s CCC: $37.00
Published on Web 08/15/2007

This architecture resembles that of the latent membrane protein 2A (LMP2A) of Epstein−Barr virus (EBV), a γ1-herpesvirus, which is a 12-transmembrane domain-containing protein with phosphotyrosine- (pTyr-) dependent SH2-binding motifs, as well as WW domain-binding sites, in its intracellular N-terminal tail (*11*, *12*). Similarly to K15, the LMP2A gene is also found at the rightmost end of the EBV genome (*13*). LMP2A is one of the genes encoded by EBV that are involved in maintaining latency in memory B cells (*14*). The N-terminal region of LMP2A binds downstream effectors of the B cell receptor (BCR), such as Lyn, which recognizes a phosphorylated LMP2A YEEA motif through its SH2 domain, and Syk, which binds a bisphosphorylated immunoreceptor tyrosine-based activation motif (ITAM) (*11*, *15*, *16*).

K15 has been implicated in both latent and lytic infection, and its primary role has therefore remained uncertain (*17*, *18*). K15 transcripts have been weakly detected in latently infected PEL cell lines and can be upregulated with lytic induction by tetradecanoylphorbol acetate (*8*, *10*, *17*, *19*). However, K15 transcription is mediated by the KSHV immediate-early protein Rta, which is consistent with expression during lytic replication of KSHV (*18*). Recent data suggest that K15 can modify specific intracellular signaling pathways through the activity of its C-terminal cytoplasmic region. For example, the K15 C-terminal tail is capable of downregulating BCR signaling, as judged by the ability of a CD8/K15 fusion protein to inhibit intracellular calcium mobilization, in a fashion that depends on the synergistic activity of the conserved PPLP and YEEV motifs in the C-terminal region (*8*). The mechanisms by which K15 exerts its effects, however, have yet to be fully deciphered. K15 has been demonstrated to activate the Ras-MAPK and NF-κB pathways and to weakly activate the JNK-SAPK pathway in 293 cells (*20*). Furthermore, protein interaction studies have revealed potential binding partners for the conserved C-terminal tail motifs. These include an interaction between the YASIL motif and the antiapoptotic protein Hax-1, of undetermined biological significance (*21*). In vitro data also show that the C-terminal region of K15 can bind TRAF 1, 2, and 3 and can be phosphorylated on the tyrosine residue of the YEEV motif by a number of the Src family kinases (Src, Hck, Lck, Fyn, and Yes) (*10*, *20*). However, there are additional conserved motifs in the C-terminal region of K15, which potentially mediate protein−protein interactions that might contribute to K15 biological activity. Notably, the PPLP motif in the C-terminal region of K15 has the potential to engage domains that recognize proline-rich sequences, such as SH3 domains. Our studies reveal that a multidomain protein involved in endocytosis, Intersectin 2, binds to the PPLP motif of the K15 C-terminal domain through its SH3-C domain. This interaction, which can be detected both in vitro and in cells, suggests a role for K15 in endocytic trafficking.

EXPERIMENTAL PROCEDURES

Antibodies, Constructs, and Other Reagents. The M2 anti-FLAG monoclonal (mAb), anti-FLAG polyclonal (pAb), and anti-golgi 58K protein (clone 58K-9) mAb antibodies were purchased from Sigma (St. Louis, MO). The anti-MYC 9E10 mAb, anti-c-MYC (A14) pAb, and anti-glutathione *S*-transferase (GST) mAb (B14) were purchased from Santa Cruz Biotechnology (Santa Cruz, CA). The anti-EEA1 mAb and anti-Lamp-1 mAb were purchased from BD Transduction Laboratories (San Jose, CA). NeutrAvidin horseradish peroxidase (HRP) was purchased from Pierce Biotechnology (Rockford, IL). The Texas Red-conjugated anti-rabbit, Alexa Fluor 488 conjugated anti-mouse and anti-goat antibodies were purchased from Molecular Probes (Eugene, OR). The goat anti-human IgM, Fc5μ fragment specific antibody was purchased from Jackson ImmunoResearch Laboratories Inc. (West Grove, PA).

Full-length K15 P allele constructs were generously provided by Dr. Jae U. Jung (Harvard Medical School, Southborough, MA). The tagged constructs to the K15 P allele and ITSN2 were generated by cloning each cDNA into V37pDNR MCS SA donor vectors and recombined by Cre recombinase into v181 pLPS-Triple Flag or v517 pLP-dMyc SD acceptor vectors (*22*) through the BD Creator DNA cloning kit (BD Biosciences, San Jose, CA).

Cell Culture. DG75, Daudi, and Ramos B cells were grown in RPMI 1640 media (Gibco BRL, Cambridge, Ontario, Canada) supplemented with 10% fetal calf serum (FCS) (Gibco BRL). 293T cells were grown in Dulbecco's modified Eagle medium (Gibco BRL) supplemented with 10% FCS.

Transfections. DG75 cells were electroporated with a BTX ECM 830 square wave electroporator (BTX, San Diego, CA) with three 225 V pulses of 8 ms pulse length at 1 s intervals. Twenty micrograms of total DNA was transfected into a cell density of $\sim 3 \times 10^7$ cells/mL. Transfected cells were resuspended in 10 mL of fresh RPMI 1640 medium and 10% FCS and incubated 48 h at 37 °C.

293T cells were transfected with poly(ethylenimine) (PEI); 30% confluent 10 cm plates were treated with a total of 10 μg of DNA in 750 μL of Optimem medium with 25 μL of PEI and incubated for 48 h at 37 °C.

K15 PPLP Peptide Synthesis. The PPLP peptide to the M allele of K15 (LARRLPPLPSRNV) was synthesized with an Applied Biosystems 431 peptide synthesizer using 9-fluorenylmethoxycarbonyl solid-phase chemistry as previously described (*12*). Briefly, the peptide was biotinylated at the N-terminus with an ϵ-aminocaproic acid linker separating the biotin and the peptide sequence. The peptide was deprotected with trifluoroacetic acid solution, with triisopropylsilane as a hydration catalyst, and precipitated on ice in *tert*-butyl ethyl ether. Crude peptide was then dried overnight in a vacuum centrifuge, rehydrated, and purified through high-pressure liquid chromatography. Mass spectrometry and amino acid analysis were used to verify the synthesis and the concentration of the peptide.

PPLP Peptide Pulldown for MS Analysis. DG75, Daudi, and Ramos cells were individually resuspended in 1% NP-40 lysis buffer supplemented with 1 mM $NaVO_4$, 1 mM phenylmethanesulfonyl fluoride, 10 μg/mL leupeptin, and 10 μg/mL aprotinin at 1×10^8 cells/mL and incubated at 4 °C for 20 min. Insoluble material was separated by centrifugation at $\sim$23000*g* for 30 min at 4 °C. Cell lysates were mixed together and precleared with streptavidin beads alone for 30 min at 4 °C. The biotinylated PPLP peptide was precoupled to streptavidin beads for 1 h at 4 °C before being incubated with precleared lysate for $\sim$1 h at 4 °C. Beads were then washed three times with 1% NP-40 lysis buffer with inhibitors, and proteins were eluted off the beads by boiling in sodium dodecyl sulfate−polyacrylamide gel electrophoresis (SDS−PAGE) sample buffer.

Running of SDS−PAGE Gels and Excision of Bands for MS Analysis. Samples were resolved on 10% SDS−PAGE minigels, and gels were washed three times for 10 min with

deionized distilled water and stained overnight with GelCode colloidal Coomassie blue reagent (MJS BioLynx, Inc., Brockville, Ontario, Canada) at room temperature. Individual bands were manually excised and transferred to a single well with an open bottom of a 96-well microtiter plate (Genomic Solutions). Excised bands were reduced with DTT, alkylated with iodoacetamide, and digested with trypsin using an Investigator Progest (Perkin-Elmer, Wellesley, MA) autodigestor. Tryptic peptides were analyzed by liquid chromatography−tandem mass spectrometry (LC-MS/MS) on a LCQ-DECA ion trap machine (Finnegan). Data were analyzed using the Sonar software (ProteoMetrics, New York, NY).

Probing SH3 Domain Protein Arrays. The SH3 domain arrays were purchased from Panomics Inc. (Redwood, CA), blocked using the Panomics SH2 domain blocking mixture (optimized solution for use with biotinylated peptides), and probed using 1 μM biotinylated peptide which was premixed with streptavidin−HRP according to manufacturer's instructions. Bound peptides were detected using chemiluminesence.

Immunoprecipitation Experiments and GST Pulldowns. Transfected cells were harvested 48 h posttransfection, washed two times with phosphate-buffered saline (PBS), and lysed in 1% NP-40 supplemented with inhibitors (see above). Insoluble material was separated by centrifugation at ~23000*g* for 15 min at 4 °C. For immunoprecipitation experiments lysates were precleared with protein G−Sepharose beads alone for 30 min before being incubated with the indicated antibody coupled to protein G−Sepharose beads for 1 h at 4 °C on a nutator. For GST fusion protein experiments equivalent amounts of lysates were incubated with ~10 μg of fusion protein coupled to beads for 1 h at 4 °C on a nutator. Immunoprecipitations and GST pulldowns were then washed three times with lysis buffer with inhibitors and eluted by boiling in SDS−PAGE sample buffer.

Western Blotting. Cell lysates, immunoprecipitations, GST, and peptide pulldowns were resolved on SDS−polyacrylamide gels, transferred to nitrocellulose membranes, and blocked in 5% skim milk powder in Tris-buffered saline containing 0.05% Tween 20 (TBST) or 5% bovine serum albumin (BSA) in TBST. Membranes were incubated with the indicated primary Ab in TBST with 5% skim milk powder either overnight at 4 °C or for 1 h at room temperature. Membranes were then washed five times for 10 min in TBST followed by incubation with a secondary Ab, either goat anti-mouse or goat anti-rabbit HRP-coupled reagent (Bio-Rad) in TBST for 1 h at room temperature. Membranes were washed five times for 10 min in TBST and rinsed once in TBS before being exposed to enhanced chemiluminescence (ECL) reagent (Pierce). Blots were stripped with TBST, pH 2, for 30 min before being reprobed as above.

Generation and Purification of GST Fusion Proteins. The K15 P allele C-terminal tail was cut out of pSL301 with *Bgl*II and *Not*I and cloned into the *Bam*HI and *Not*I sites of pGEX4T1 (Pharmacia). The resulting cDNA encoding the GST-K15 C-terminal tail fusion (GST-K15) was used to transform BL21 competent cells, and fusion protein was purified with glutathione−Sepharose (Pharmacia, Baie d'Urfe, Quebec, Canada). The purified fusion protein was run out on 12% SDS−PAGE gels and quantified against BSA standards.

GST fusion proteins were generated to the individual SH3 domains of ITSN2 as well as all five together by subcloning into the pGEX4T1 vector. Oligonucleotides were synthesized with 5′ *Eco*RI and 3′ *Xho*I restriction enzyme sites and used to generate PCR products to SH3-A (aa 730−790), SH3-B (aa 870−928), SH3-C (aa 954−1011), SH3-D (aa 1025−1089), SH3-E (aa 1099−1158), and SH3A-E (aa 730−1158). Products were digested with *Eco*RI and *Xho*I restriction enzymes and cloned into the corresponding sites of the pGEX4T1 vector. GST fusion proteins were expressed and purified from BL21 competent cell lysates with glutathione−Sepharose beads (Amersham). Eluted fusion proteins were dialyzed in PBS and stored at −80 °C.

Synthesis and Blotting of SPOTS Membranes. SPOTS membranes were synthesized as previously described (*23*). Membranes were blocked with 5% skim milk powder in TBST and probed with GST-SH3A-E (0.1 μM in TBST) at 4 °C on a nutator overnight. Membranes were washed five times for 10 min the following day and incubated with HRP-conjugated anti-GST mAb (B14) (Santa Cruz) for 1 h at room temperature. Membranes were subsequently washed five times for 10 min and visualized by exposure to ECL reagent.

Binding Analysis Using Surface Plasmon Resonance (SPR). The ITSN2 SH3 domains A−E were immobilized by using standard amine-coupling chemistry to a level of 2469 (SH3-A), 2132 (SH3-B), 1158 (SH3-C), 1861 (SH3-D), and 1954 (SH3-E) response units (RU; 250 pg/mm^2) onto a CM4 chip using a Biacore 3000 biosensor (Biacore AB, Uppsala, Sweden). Peptides were serially diluted in running buffer HBS-EP [10 mM Hepes, pH 7.4/150 mM NaCl/3 mM EDTA/0.005% polysorbate 20 (v/v)] (Biacore AB). For association phases, 100 μL of peptide was injected at a fast flow rate (100 μL/min) over both flow cells, and dissociation phases were monitored for up to 200 s by injecting HBS-EP only. Sensorgram deviations introduced by system noise were subtracted by using a second referencing sensorgram made from a 100 μL HBS-EP injection (*24*). Equilibrium binding responses were fitted using a standard Michaelis−Menten equation to determine the K_D. To demonstrate reproducibility, sensorgrams of multiple concentrations of peptide, each performed in quadruplicate, were overlaid (see Figure 5B).

Subcellular Fractionation. All sucrose solutions were made in 20 mM Tris, pH 7.2, with 0.5 mM EDTA. Transfected cells were harvested 48 h posttransfection and resuspended in 1.5 mL of 5% sucrose supplemented with inhibitors (see above). Cells were then homogenized through a 26G syringe needle (>35 strokes) on ice and centrifuged at 2500 rpm for 5 min at 4 °C. Postnuclear supernatant was layered onto a 10 mL continuous sucrose gradient of 5−45%. Organelles were resolved by ultracentrifugation at 27700 rpm for 110 min at 4 °C using the Beckman L8-80M Ultracentrifuge SW-41 Ti rotor (Beckman, Palo Alto, CA). Fractions of 0.5 mL were extracted and resolved on 12% SDS−PAGE gels.

Immunofluorescence. Glass coverslips were treated with 1 M HCl overnight before being coated with poly(L-lysine) for 30 min. An aliquot of transfected DG75 cells was added to coated coverslips for 10 min at room temperature. Adhered cells were fixed in 4% paraformaldehyde for 20 min at 4 °C and permeabilized with 0.5% Triton X-100 for 5 min. Coverslips were blocked in 5% BSA in PBS overnight before being stained with primary antibodies in blocking buffer for >1 h. Staining with anti-FLAG pAb was detected with Texas Red-conjugated anti-rabbit immunoglobulin (Ig), and anti-MYC 9E10 was detected with Alexa Fluor 488 conjugated anti-mouse Ig. Coverslips were mounted with Geltol mounting medium. Cells were imaged on the Deltavision deconvolution microscope (Applied Precision Inc., Issaquah, WA) equipped with the Olympus 100× (NA 1.35) objective lens and softWoRx software as described in ref *25*.

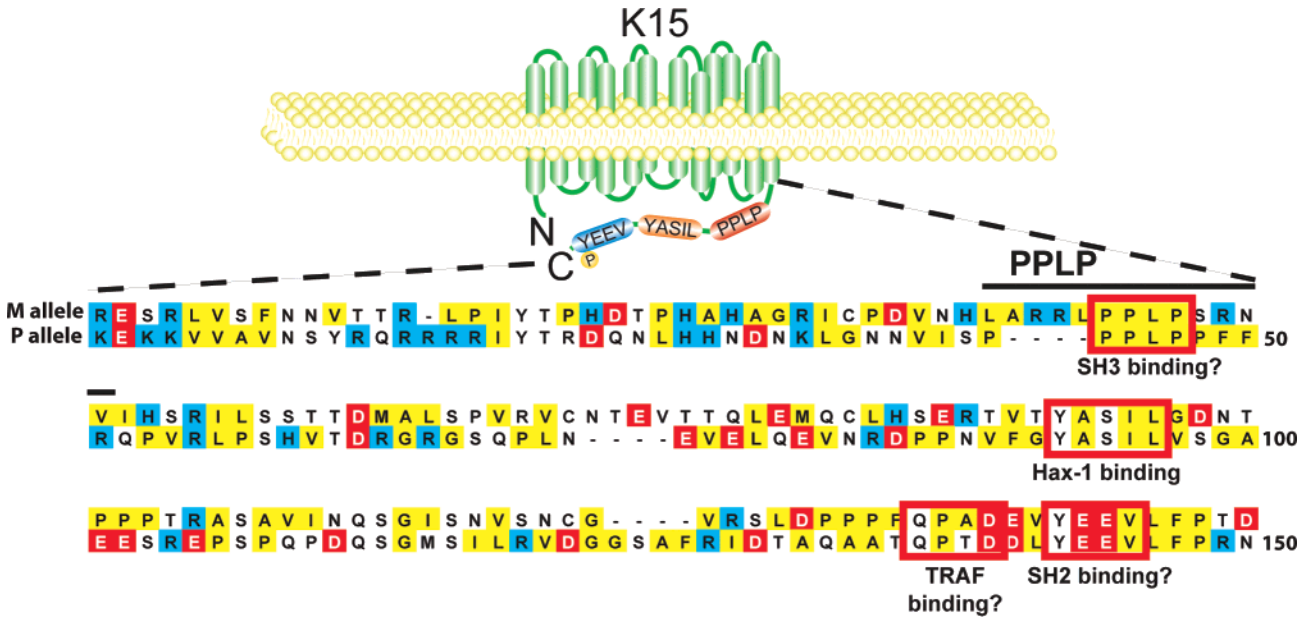

FIGURE 1: Sequence alignment of the carboxy-terminal cytoplasmic tail of the K15 P and M alleles. The conserved putative SH3-binding, SH2-binding, TRAF-binding and YASIL motifs are indicated by red boxes. The 13-residue PPLP peptide from the K15 M allele used for precipitation experiments and probing of domain arrays is indicated by a bold line. Yellow boxes represent nonpolar residues, red boxes represent acidic residues, blue boxes represent basic residues, and clear boxes represent polar uncharged residues. Complete alignment was performed using ClustalX (version 1.83).

BCR Internalization Assay. Transfected DG75 cells were harvested 48 h posttransfection and resuspended in cold sorter buffer (1% FCS in PBS). 1×10^6 cells were resuspended in 50 μL of 100 μg/mL goat anti-IgM antibody in sorter buffer and placed on ice for 15 min. Antibody-bound cells were then stimulated for up to 60 min at 37 °C. Stimulations were terminated and washed twice with cold sorter buffer. Stimulated cells were then resuspended in 50 μL of 30 μg/mL Alexa Fluor 488 conjugated anti-goat Ig on ice and placed in the dark for 45 min. Labeled cells were washed twice with cold sorter buffer, fixed with 4% PFA, and analyzed using a FACScaliber cell sorter (Becton Dickinson, Palo Alto, CA).

RESULTS

Screening for Interacting Proteins of the K15 PPLP. To identify proteins that associate with the conserved PPLP motif in the C-terminal tail of K15, a biotinylated 13 amino acid peptide (LARRLPPLPSRNV) comprising this sequence was synthesized (Figure 1). Due to the relative insolubility of the PPLP peptide from the K15 P allele, we used a peptide corresponding to the PPLP sequence of the K15 M allele (Figure 1). The peptide was immobilized on streptavidin beads and used to affinity purify proteins from cell lysates of a number of human B cell lines, including DG75, Daudi, and Ramos. Precipitated cellular proteins were resolved on a SDS−PAGE gel and visualized with colloidal Coomassie blue stain (Figure 2). Proteins specifically precipitated by the PPLP peptide, but not beads alone, were excised from the gel and identified by liquid chromatography−tandem mass spectrometry (LC-MS/MS) (Table 1). Intriguingly, all of the proteins identified as selectively binding the PPLP sequence (Intersectin 2, Epsin15-related protein, Pacsin 2, and clathrin heavy chain) have been previously described to regulate endocytic trafficking of receptors (*26*−*29*). Two of these proteins, Intersectin 2 and Pacsin 2, have SH3 domains that could directly bind to the PPLP peptide and are both involved in regulating intracellular trafficking by inhibiting endocytosis via their SH3 domains (*26*, *28*). Both proteins

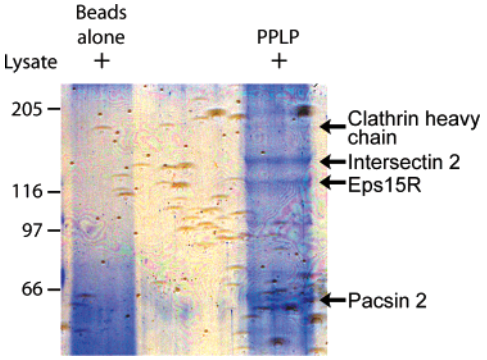

FIGURE 2: The PPLP motif of K15 interacts with SH3 domain-containing proteins involved in endocytosis. Lysates from DG75, Daudi, and Ramos cell lines were mixed and precleared with streptavidin beads alone (lane 1) before incubation with the biotinylated PPLP peptide (lane 2) as described in Experimental Procedures. Precipitated proteins were resolved by SDS−PAGE and visualized with colloidal Coomassie blue stain. Unique bands in lane 2 (indicated by arrows) were excised from the gel and identified by LC-MS/MS. Molecular mass markers (in kilodaltons) are indicated on the left of the gel.

can also interact with a similar set of binding partners, including dynamin, synaptojanin, and WASP, through their SH3 domains (*30*, *31*). Furthermore, the Epsin15-related protein (Eps15R), which was also precipitated by the K15 PPLP peptide, complexes with a number of endocytic proteins, including Intersectin proteins, to control clathrin-mediated endocytosis (*27*, *32*). Thus, the PPLP motif of K15 interacts with proteins associated with endocytosis, several of which possess SH3 domains. We therefore examined if the SH3 domains of Intesectin 2 or Pacsin 2 could interact directly with the PPLP motif of K15 and explored the more global SH3 domain-binding properties of this peptide.

The Conserved PPLP Motif in K15 Is an SH3 Domain-Binding Sequence. To determine if the K15 PPLP peptide associates with Intersectin 2 and Pacsin 2 via their SH3 domains, the biotinylated PPLP peptide was used to probe

Table 1: Proteins Identfied by Mass Spectrometry as Interacting with the Conserved PPLP Motif of the K15 M Allele

protein	accession (Gl)	peptide sequence determined	residues
clathrin heavy chain	4758012	SVDPTLALSVYLR	469−481
Intersectin 2	22325383	QLQQELQEYQNK	207−231
		AGQPLPLTLPPELVPPSFR	313−331
		RQELLNQK	466−473
		AQSLIDLGSSSSTSSTASLSGNSPK	538−549
Eps15R	10864047	DQFALAMFIQQK	286−300
		TDLDLDGYVSGQEVK	331−343
		ELDDISQEIAQLQR	385−398
		LQQEETQLEGSIQAGR	508−523
		STQDEINQAR	535−544
Pacsin 2	6005826	AYAQQLTEWAR	54−64
		AIYHDLEQSIR	265−275
		ALYDYEGQEHDELSFK	443−448
		LDNGQVGLYPANYVEAIQ	469−486

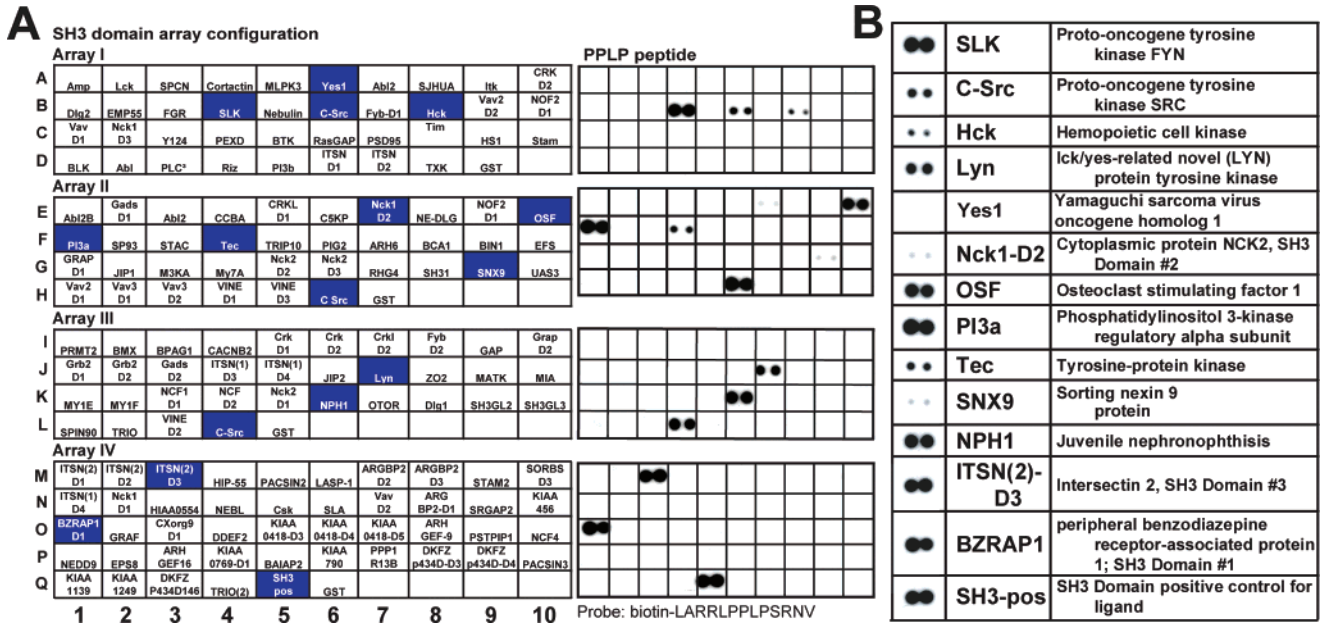

FIGURE 3: The PPLP motif of K15 binds selectively to certain SH3 domains. (A) SH3 domain array membranes were incubated with 1 μM biotinylated PPLP peptide conjugated to streptavidin−HRP at room temperature for 1 h, after being prepared as described in Experimental Procedures. Bound peptides were analyzed by chemiluminescence using TranSignal detection buffers. SH3 domains recognized by the PPLP peptide are labeled with a blue box (left side) with the corresponding duplicate spots (right side). (B) Full names of the interacting SH3 domain-containing proteins with their corresponding duplicate spots on the left.

four arrays containing a total of 150 human SH3 domains (Figure 3A). We have previously found that many of the SH3 domains in these arrays are active in peptide binding and show reproducible selectivity for specific peptide ligands. However, we cannot exclude the possibility that a minority of the domains are not properly folded (*33*). The results show that the PPLP peptide recognizes a limited set of SH3 domains in this array-based format, with varying affinities (Figure 3). The SH3-C domain of Intersectin 2 was among those that bound the biotinylated PPLP peptide (Figure 3B). This suggests that the interaction between Intersectin 2 and the PPLP peptide identified in the pulldown experiments (see Figure 2) is due to a direct, SH3 domain-dependent interaction. In contrast, the PPLP peptide did not bind the SH3 domain of Pacsin 2 on the array (Figure 3A, box M5). Given that Intersectin 2 has the potential to directly associate with K15, we investigated whether this interaction occurs in cells.

K15 Interacts with the Clathrin-Associated Endocytic Protein Intersectin 2 in Vitro and in Cells. The involvement of K15 in intracellular trafficking remains unexplored. However, the number of endocytic proteins identified as interacting with the K15 PPLP motif by mass spectrometry suggests a possible role for K15 in regulating the endocytic machinery. Intersectin 2 (ITSN2) is a multifunctional adaptor protein that regulates endocytosis and possesses several signaling domains (*26*, *30*) (Figure 4A). These include two N-terminal Eps15 homology domains (EH), a central coiled-coil (CC) domain, and five tandem SH3 domains. A longer isoform of ITSN-2, ITSN2-L, also has a Dbl homology (DH) domain, which acts as a Rho guanine nucleotide exchange factor, a Pleckstrin homology (PH) domain, and a C2 domain. On the basis of its apparent molecular mass, the ITSN2 shorter isoform was precipitated by the PPLP peptide from B cell lysates. To pursue the interaction between K15 and Intersectin-2, we constructed a GST fusion protein comprising the C-terminal cytoplasmic tail of the K15 P allele and examined its ability to precipitate Myc-tagged ITSN2 from a 293T cell lysate (Figure 4B, upper panel). The resulting data showed that Myc-tagged ITSN2 was indeed specifically precipitated by the C-terminal tail of K15.

We also examined if K15 and ITSN-2 could interact in cells. To this end, a triply Flag-tagged K15 polypeptide (C-

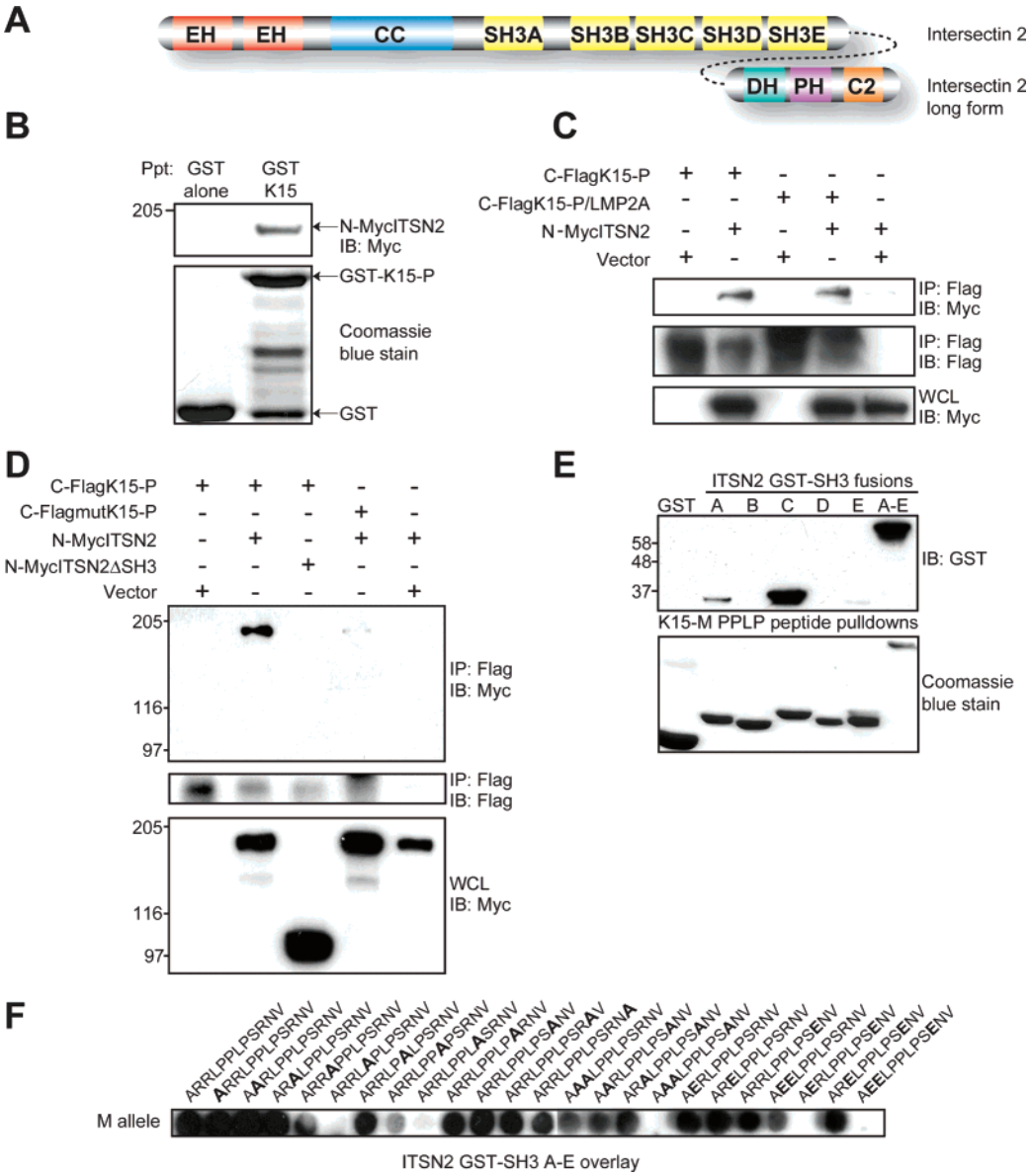

FIGURE 4: K15 associates with the SH3 domains of the endocytic adaptor protein, Intersectin 2 (ITSN2), through its PPLP motif. (A) Domain architecture of ITSN2. The long isoform of ITSN2 has a C-terminal extension as shown by the dotted line. (B) 293T cells were transfected with 10 μg of MYC-tagged ITSN2 (N-MycITSN2) and incubated at 37 °C for 48 h. Cell lysates were incubated with a GST fusion protein to the C-terminal tail of the K15 P allele (GST-K15-P), and precipitating ITSN2 was analyzed by immunoblotting with the anti-MYC 9E10 mAb (upper panel). Coomassie blue staining of purified GST and GST-K15-P separated on an SDS−PAGE gel to show equal amounts of fusion protein was used for pulldowns (lower panel). (C) DG75 B cells were electroporated with a total of 20 μg of the indicated plasmids (10 μg of each) and incubated at 37 °C for 48 h. Cell lysates were immunoprecipitated with the M2 anti-FLAG mAb, and precipitating ITSN2 was analyzed by immunoblotting with the anti-c-MYC (A-14) pAb (upper and bottom panel). Blots were reprobed with the M2 anti-FLAG mAb to analyze K15 and LMP2A/K15 expression (middle panel). (D) DG75 B cells were electroporated with 10 μg of each of the indicated plasmids and incubated at 37 °C for 48 h. Cell lysates were immunoprecipitated with the M2 anti-FLAG mAb, and precipitating ITSN2 or ITSN2ΔSH3 was analyzed by immunoblotting with the anti-c-MYC (A-14) pAb (upper and bottom panel). Blots were reprobed with the M2 anti-FLAG mAb to analyze K15 and mutK15 expression (middle panel). (E) GST alone or the indicated GST-SH3 domains of ITSN2 were precipitated with the biotinylated K15 M allele PPLP peptide coupled to streptavidin beads. Precipitating fusion proteins were analyzed by immunoblotting with the anti-GST (B-14) HRP mAb (upper panel). Fusion proteins were separated on SDS−PAGE gels and visualized with Coomassie blue stain for equal expression levels (lower panel). (F) 12-mer peptides, each with single, double, or triple substitutions to alanine or glutamate (in bold), were generated to the PPLP region of the K15 M allele sequence on a SPOTS membrane. Membranes were probed with 0.1 μM GST fusion protein to all five SH3 domains of ITSN2 (GST-SH3 A-E). Bound fusion proteins were analyzed with the anti-GST (B-14) HRP mAb.

Flag K15-P) or a triply Flag-tagged fusion protein comprising the transmembrane domains of the EBV protein LMP2A fused to the N-terminal and C-terminal tails of K15 (C-Flag-K15-P/LMP2A) was tested for its ability to coimmunoprecipitate with a Myc-tagged ITSN2 from DG75 B cell lysates (Figure 4C, upper panel). These results show that both the Flag-tagged K15 P allele and K15/LMP2A fusion coprecipitated with ITSN2. To determine how ITSN2 and K15 interact in cells, we mutated the prolines of the PPLP motif to glycines, in the context of the Flag-tagged K15 (C-FlagmutK15-P). Conversely, we investigated if the SH3 domains of ITSN2 are required for interaction with K15 by using an ITSN2 protein lacking all five SH3 domains (N-Myc-ITSN2ΔSH3). We found that while the Flag-tagged

K15 and Myc-tagged ITSN2 proteins coimmunoprecipitated from DG75 B cells, mutation of either the K15 PPLP motif or deletion of the ITSN2 SH3 domains abolished the ability of these proteins to stably associate in cells (Figure 4D, upper panel). This supports the notion that the interaction between K15 and ITSN2 is mediated by the SH3 domains of ITSN2 and the PPLP motif of K15. Since ITSN2 has five SH3 domains that could potentially bind the PPLP motif in K15, we examined the ability of GST fusion proteins containing each of the individual SH3 domains of ITSN2 or a GST fusion protein comprising all five SH3 domains of ITSN2 to interact with the biotinylated K15 M allele PPLP peptide (Figure 4E, upper panel). The peptide preferentially precipitated the SH3-C domain of ITSN2, and this selectivity is in agreement with data obtained by probing SH3 domain arrays (see Figure 3).

To identify the key residues in the PPLP motif required for interaction with the SH3 domains of ITSN2, we synthesized variant peptides of the PPLP motif of the K15 M allele on a membrane in which each residue of the peptide was substituted individually with alanine. The 12-mer peptides consisted of 12 amino acids from the K15 M allele with four residues N-terminal and C-terminal to the PPLP motif (ARRLPPLPSRNV). These peptides were probed with a GST fusion protein containing the five SH3 domains of ITSN2. This analysis showed that the first and last prolines of the PPLP motif were required for the binding of the SH3 domains of ITSN2. Thus, the PPLP motif of K15 apparently behaves as the canonical SH3 domain-binding PXXP motif (*34*, *35*) (Figure 4F). Basic residues, such as arginine and lysine, are often observed N-terminal (class I) or C-terminal (class II) to the SH3-binding PXXP consensus sequence. To test whether the three arginine residues flanking the PPLP motif in the K15 M allele are important for interaction with the SH3 domains of ITSN2, we analyzed PPLP peptides with single, double, or triple substitutions of these arginines with alanine. The presence of any one of the flanking arginines was sufficient for binding to the ITSN2 SH3 domains, but a peptide lacking all three arginines failed to bind. Similar data were obtained with arginine-to-glutamate substitutions, except that a mutant that only retained the second arginine (i.e., AERLPPLPSENV) did not bind (Figure 4F). Taken together, these data show that K15 and ITSN2 associate in cells in a fashion that requires the SH3-C domain of ITSN2 and the PPLP motif of K15. Binding of the PPLP motif required the canonical proline residues (*P*PL*P*) and at least one flanking arginine, raising the possibility that it may bind in both class I and class II orientations.

Surface Plasmon Resonance Analysis Reveals That the SH3-C Domain of ITSN2 Preferentially Binds the K15 PPLP Motif. To further investigate the preferential binding of the SH3-C domain of ITSN2 to the PPLP sequence of K15 and pursue the physiological relevance of this interaction, we examined the affinity of the interaction using surface plasmon resonance (SPR) technology. For this purpose, each ITSN2 SH3 domain was immobilized on a BIACORE chip and probed with varying concentrations of PPLP peptide. Consistent with the peptide pulldown data, the SH3-C domain interacted more strongly with the K15 peptide, with a K_D of 13.5 μM (Figure 5D). This affinity is characteristic of other SH3 domains for PXXP motifs. The PPLP peptide interacted very weakly with the SH3-A (K_D = 280.7 μM) and SH3-E (K_D = 254.6 μM) domains and with even lower affinity to the SH3-B (K_D = 1.833 mM) and SH3-D (K_D = 1.519 mM) domains (Figure 5D). These data provide further support for our findings that the interaction between K15 and ITSN2 is mediated by preferential binding of the K15 PPLP motif to the SH3-C domain of ITSN2.

K15 Colocalizes with ITSN2 in DG75 B Cells. K15 has been previously reported to localize to a perinuclear region including the golgi and ER (*8*, *21*), whereas ITSN2 has been suggested to be evenly distributed throughout the cytoplasm (*26*). Overexpression of intersectin has also been shown to regulate the localization of binding proteins into circular structures within Cos cells (*32*). To further assess the interaction between K15 and ITSN2 in B cells, we analyzed their localization within the cell by subcellular fractionation. Previous studies have demonstrated that K15 localizes to lipid rafts as seen by blotting for caveolin-1 (*20*). To identify the cellular compartments containing K15 and ITSN2, we separated intact organelles along a continuous sucrose gradient as described in Experimental Procedures. Lysates prepared from DG75 cells expressing C-FlagK15-P and N-MycITSN2 were resolved along a 5−45% sucrose gradient by ultracentrifugation. Western analysis showed that K15 and ITSN2 localize to the same fractions as the early endosomal antigen 1 (EEA1) and overlap with the golgi fractions identified with a golgi 58K marker (Figure 6). These data are consistent with a significant colocalization of KSHV K15 and ITSN2. However, the distributions of the two proteins do not fully overlap, suggesting that there are regions within the cell that they are not associated. We also noted that the BCR is found in similar fractions as K15, which suggests that K15 may directly affect BCR function.

These data were complemented by immunofluorescence experiments, in which N-MycITSN2 was cotransfected with C-FlagK15-P or C-FlagmutK15-P into DG75 B cells. Cells were immunostained with anti-Flag or anti-Myc antibodies, followed by fluorescence-conjugated secondary antibodies, and visualized by deconvolution microscopy. C-FlagK15-P and C-FlagmutK15-P, as well as the MycITSN2, all showed a punctate staining pattern (Figure 7). The staining patterns of the two proteins showed that K15 and ITSN2 were colocalized in specific cytoplasmic regions within the cell, which is consistent with the fractionation experiments. In contrast, C-FlagmutK15-P showed little overlap with N-MycITSN2 by immunofluorescence. These data argue that K15 and ITSN2 associate in discrete punctate regions of cells and that this colocalization shows a significant dependence on the interaction between the K15 PPLP motif and the ITSN2 SH3 domains.

K15 and ITSN2 Regulate the Rate of BCR Internalization. The signaling motifs within the C-terminal domain of K15 have been previously shown to alter BCR function (*8*). The preceding data indicate that the K15 PPLP motif interacts with components of the endocytic machinery and suggest that full-length K15 is found in similar fractions as the BCR. We therefore investigated whether K15 may alter internalization of the BCR. The effect of ITSN2 on BCR internalization was analyzed by overexpressing ITSN2 in DG75 B cells. Cells were stimulated at 37 °C with an anti-human IgM antibody for up to 60 min, and remaining surface BCR was visualized with an Alexa 488 conjugated secondary antibody by flow cytometry as described in Experimental Procedures.

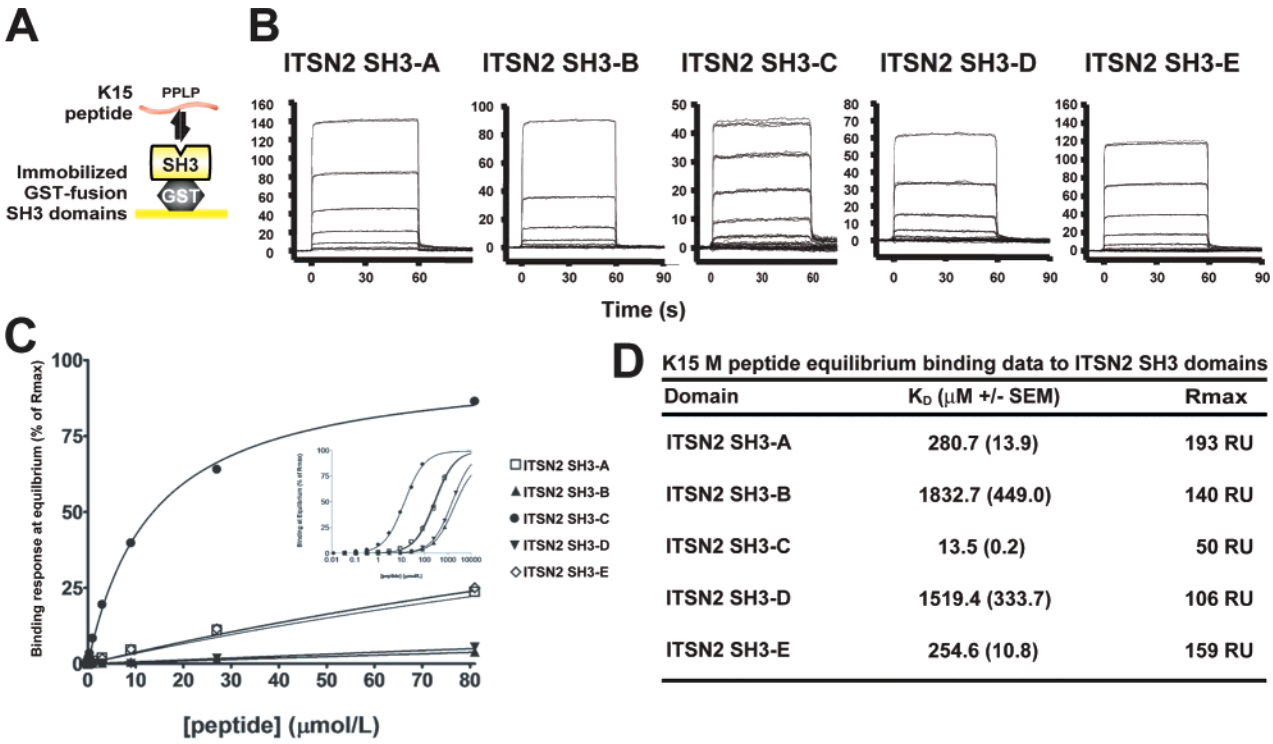

Domain	K_D (μM +/- SEM)	Rmax
ITSN2 SH3-A	280.7 (13.9)	193 RU
ITSN2 SH3-B	1832.7 (449.0)	140 RU
ITSN2 SH3-C	13.5 (0.2)	50 RU
ITSN2 SH3-D	1519.4 (333.7)	106 RU
ITSN2 SH3-E	254.6 (10.8)	159 RU

FIGURE 5: The third SH3 domain of ITSN2 binds with highest affinity to the PPLP motif of the K15. (A) Schematic of the K15 PPLP peptide binding to immobilized GST fusion protein on a flow cell chip for BIACORE analysis. (B) Sensorgram data for the equilibrium binding experiments for each SH3 domain as measured by binding response units. Each SH3 domain of ITSN2, as a GST fusion protein, was immobilized onto the BIACORE CM4 chips by amine coupling. The biotinylated K15 M allele PPLP peptide was passed over this chip at a series of concentrations ranging from 37 nM to 2.2 mM (except SH3-C which had a maximum peptide concentration of 81 μM) in a 3-fold dilution series. Each equilibrium binding curve was performed in quadruplicate for every peptide concentration. (C) Normalized binding data of the ITSN2 SH3 domains to the K15 M allele PPLP peptide representing up to 81 μM peptide concentration. The inset shows the full data set with the peptide concentration on the *x*-axis shown on a logarithmic scale. The *y*-axis on each graph represents binding at equilibrium normalized to a calculated R_{max} value. The K_D was determined using nonlinear fitting of the normalized equilibrium binding responses using the standard Michaelis−Menten equation. (D) Equilibrium binding data (K_D) of each SH3 domain to the K15 PPLP peptide. R_{max} values give the theoretical maximum binding capacity of the peptide as measured by the amount of fusion protein immobilized.

In cells that overexpressed ITSN2, there was an inhibition of BCR internalization (Figure 8A). These data are consistent with previous literature showing that ITSN2 can inhibit transferrin uptake (*26*) and that overexpression of ITSN SH3 domains inhibits endocytosis (*36*). Furthermore, K15 or mutK15 was transfected into DG75 B cells. In cells expressing K15 there was an increase in the rate of BCR internalization in comparison to empty vector control, consistent with the view that K15 alters BCR trafficking (Figure 8B). In cells expressing the mutant form of K15 this stimulation of BCR internalization appeared to be attenuated, although these results did not reach statistical significance for all time points. A plausible explanation is that the PPLP motif acts redundantly with the YEEV motif to regulate BCR function (*8*).

DISCUSSION

Viral and bacterial pathogenic proteins frequently modify the behavior of infected cells through motifs that recruit the interaction domains of intracellular polypeptides. Previous work with the LMP2A protein of EBV has provided evidence for such viral-cell protein interactions, through the recruitment of proteins with SH2 and WW domains to tyrosine phosphorylated and proline-rich sites (*11*, *15*, *16*, *37*). These studies have led us to investigate the biochemical function of the structurally similar protein, K15, of KSHV.

It has been proposed that K15 elicits biological responses through the conserved PPLP, YASIL, and YEEV motifs within its cytoplasmic C-terminal tail; however, there have been no reports on proteins that interact with the K15 PPLP motif. To further understand K15's interactions with host cells, we identified proteins with the capacity to interact with this proline-rich sequence. By screening for proteins that interact with the PPLP motif using mass spectrometry analysis (Figure 2) as well as SH3 domain arrays (Figure 3), we identified a novel interaction between K15 and the adaptor protein ITSN2 that suggests a possible role for K15 in endocytosis.

The analysis of B cell proteins that bind the PPLP motif by mass spectrometry yielded four interacting proteins, all of which are components of the endocytic machinery. These included SH3 domain-containing proteins ITSN2 and Pacsin 2 as well as the trafficking proteins Eps15R and clathrin (Figure 2). These data suggested that the PPLP motif binds a subset of SH3 domains that recognize the PXXP consensus amino acid sequence. The proteins Eps15R and clathrin lack SH3 domains, which suggests their association with the K15 PPLP peptide is indirect and likely in complex with other SH3 domain-containing endocytic proteins. As a second approach we used a biotinylated PPLP peptide motif to probe 150 arrayed SH3 domains and identified 13 interacting SH3 domains (Figure 3). Among these, the only SH3 domain from a protein that also precipitated with the PPLP peptide from a B cell lysate was the SH3-C domain of ITSN2. We confirmed that a GST fusion containing the C-terminal tail

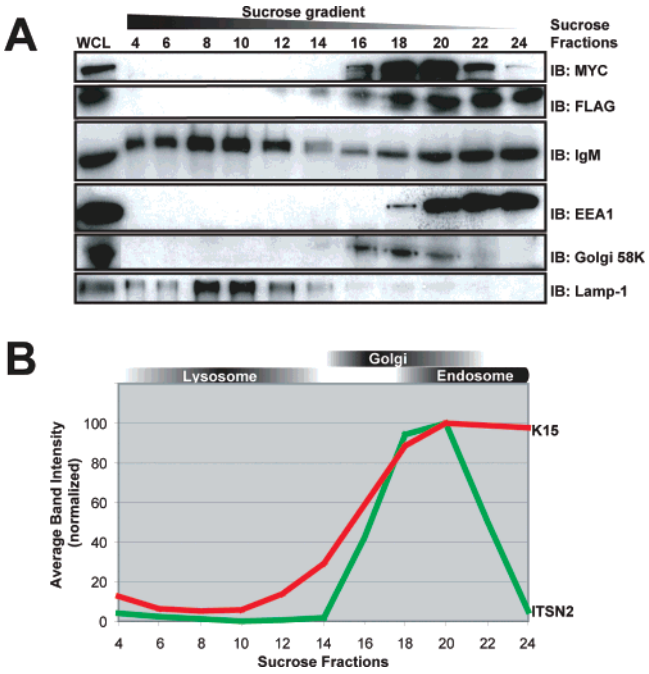

FIGURE 6: K15 and ITSN2 are found in endosomal and golgi compartments within DG75 B cells. (A) Lysates from DG75 cells electroporated with a total of 20 μg of N-MycITSN2 and C-FlagK15-P were separated along a 5−45% continuous sucrose gradient by ultracentrifugation at 27700 rpm for 110 min at 4 °C. 0.5 mL fractions and whole cell lysates were separated by SDS−PAGE and analyzed by immunoblotting with the anti-MYC 9E10 mAb (upper panel), M2 anti-FLAG mAb (second panel), goat anti-human IgM antibody (third panel), anti-EEA1 mAb (fourth panel), anti-golgi 58K protein (58K-9) mAb (fifth panel), and anti-Lamp-1 mAb (bottom panel). (B) Fraction bands from the N-MycITSN2 (green) and C-FlagK15-P (red) blots were quantified using Bio-Rad quantity one 1-D analysis software (version 4.5.2). Band intensities were normalized to the maximum band intensity of each condition.

of K15 associates with ITSN2 (Figure 4) but not with full-length Pacsin 2 (data not shown). Furthermore, we demonstrated that full-length K15 and ITSN2 proteins coprecipitate from transfected DG75 B cells (Figure 4).

Human ITSNs, including ITSN1 and ITSN2, are large scaffolding proteins that are responsible for the assembly of protein complexes involved in the clathrin-mediated endocytic machinery (*26*, *38*). Both ITSN proteins can be expressed as a short isoform or a long isoform with C-terminal DH, PH, and C2 domains. Our data demonstrate the expression of the shorter isoform of ITSN2 in human B cells (Figure 2). The N-terminal EH domains of ITSN1 and ITSN2 are protein−protein interaction domains that typically bind NPF motifs in other proteins involved in endocytic trafficking proteins (*30*, *39*). The ITSN coiled-coil region interacts with Eps15, SNAP-25/23, and with ITSN itself (*30*, *32*, *40*). The SH3 domains of ITSN have been reported to interact with dynamin, synaptojanin, Sos, and WASp (*32*, *41*, *42*). Furthermore, SH3-C, SH3-E, and especially SH3-A have also been shown to inhibit endocytosis (*36*). This effect is also observed in B cells, since the internalization of the BCR upon anti-IgM stimulation is inhibited in cells overexpressing ITSN2 (Figure 8A).

The SH3-C domain of ITSN2 binds the K15 PPLP peptide with a dissociation constant of 13.5 μM (Figure 5), which is in the affinity range with which SH3 domains typically bind

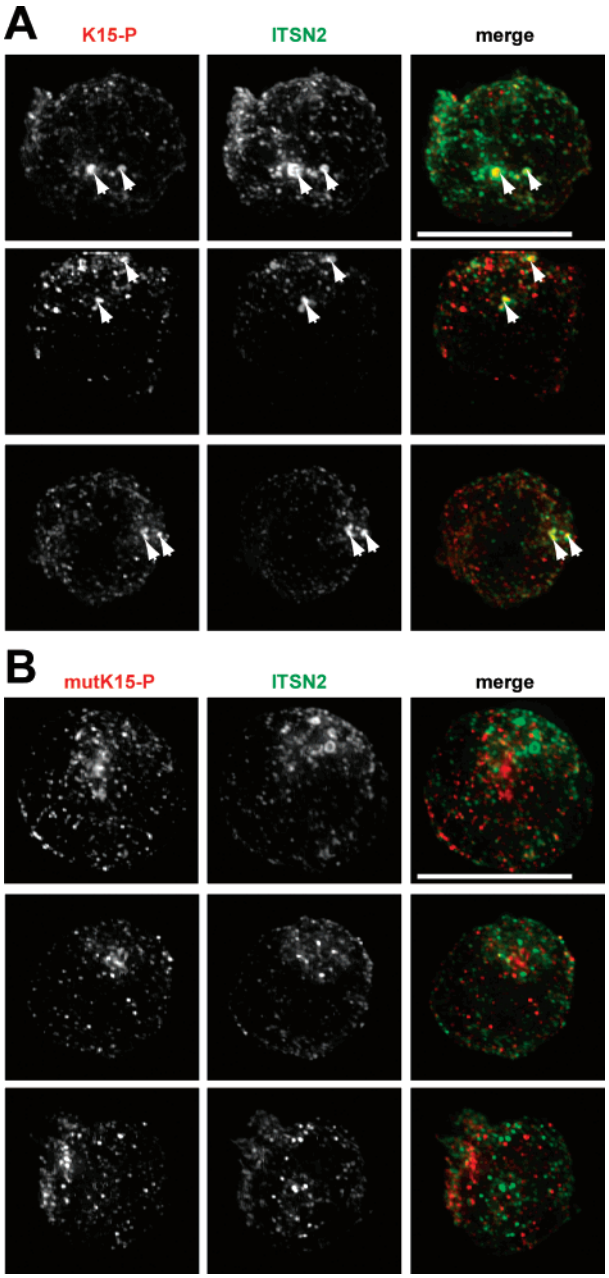

FIGURE 7: K15 and ITSN2 colocalize to discrete regions in DG75 B cells. DG75 cells were electroporated with a total of 20 μg of N-MycITSN2 and (A) C-FlagK15-P or (B) C-FlagmutK15-P. Cells were adhered to poly(L-lysine)-coated coverslips 48 h posttransfection. Fixed cells were permeabilized with 0.5% Triton X-100 for 5 min before they were stained with the anti-FLAG pAb and the anti-MYC 9E10 mAb for ~1 h. C-FlagK15-P or C-FlagmutK15-P and N-MycITSN2 were visualized by deconvolution microscopy with goat anti-rabbit Texas Red and goat anti-mouse Alexa 488 antibodies, respectively. Regions of colocalization are indicated with arrows. Scale bars, 10 μm.

PXXP motifs (*43*, *44*). This apparently represents selective binding, as the SH3-C and SH3-E domains of ITSN2 have been reported to bind the Wiskott−Aldrich syndrome protein (WASp) (*42*); we have confirmed these results and also observe binding of the ITSN2 SH3-A domain to WASp (unpublished results). These results suggest that the viral K15 protein has evolved specific SH3-binding activity by the acquisition of the PPLP sequence. Since ITSN2 is associated with the endocytic machinery, the interaction between K15

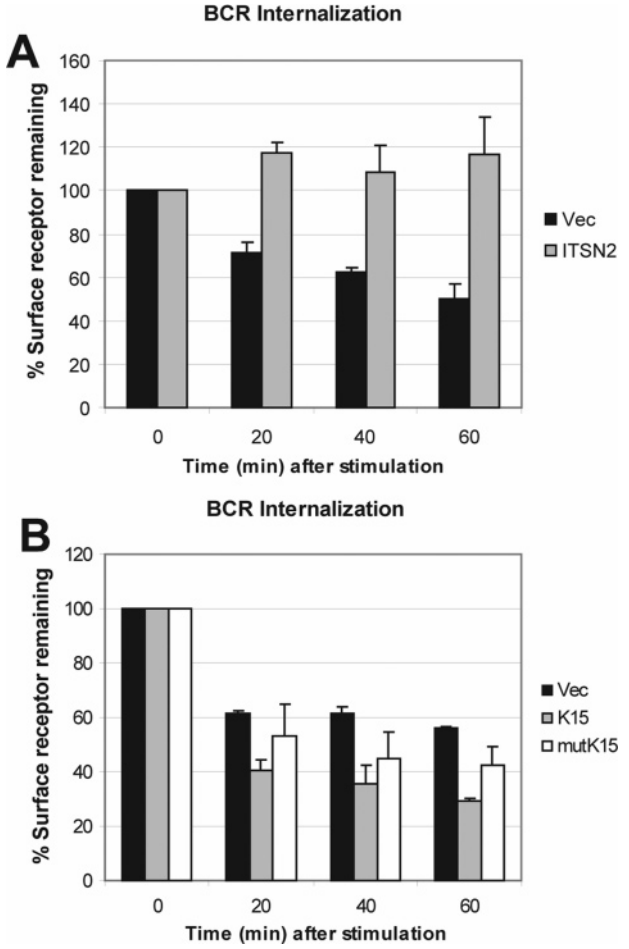

FIGURE 8: K15 increases the rate of internalization of the BCR. DG75 cells electroporated with (A) 20 μg of N-MycITSN2 or an empty vector or (B) C-Flag K15-P, C-FlagmutK15-P, or an empty vector were stimulated with goat anti-human IgM antibody for up to 60 min at 37 °C. Stimulations were stopped by cold sorter buffer, and remaining surface BCRs were stained with donkey anti-goat Alexa 488 secondary antibody for 45 min on ice. Stained cells were fixed by 4% PFA and analyzed by flow cytometry. Fluorescence intensities were normalized to the zero stimulation time point. Data shown are an average of three independent experiments.

and ITSN2 suggests the possibility that K15 affects endocytic trafficking in KSHV-infected cells.

Previous studies have shown that viral proteins can exploit host proteins to engage the endocytic machinery. As one example, the HIV-1 $Pr55^{gag}$ protein interacts with the tumor susceptibility gene 101 (tsg101) host protein to promote virion budding (*45*, *46*). Other studies have demonstrated that viral proteins, such as the KSHV K3 and K5 proteins, utilize the host ubiquitin-proteasome system to regulate internalization of membrane complexes (*47*). Our results suggest that K15 engages components of the machinery involved in clathrin-mediated endocytosis.

Consistent with this hypothesis, subcellular fractionation data suggest that K15 localizes with ITSN2 in endosomal compartments (Figure 6). In support of these findings, immunofluorescence data show K15 and ITSN2 associate specifically into discrete vesicular structures in the cytoplasmic regions within B cells (Figure 7). These images, along with the fractionation and biochemical data, also suggest that this colocalization is dependent on the interaction between the K15 PPLP motif and the ITSN2 SH3-C domain. The SH3 domains of ITSN can inhibit endocytosis, and ITSN2 itself has been proposed to inhibit receptor uptake (*26*, *36*). FACS analyses show that ITSN2 overexpression has an inhibitory effect on BCR internalization (Figure 8A). Accordingly, the K15−ITSN2 interaction links K15 to the regulation of surface expression of receptors, such as the BCR that cofractionates with K15 (Figure 6). Our experiments therefore suggest that K15 may play a role in BCR signaling by increasing its rate of internalization upon stimulation (Figure 8B). This leads us to hypothesize that the reported ability of K15 to inhibit BCR signaling may involve effects on intracellular trafficking. The mutant form of K15 lacking the PPLP motif retains some ability to affect the rate of BCR internalization, which suggests the various K15 C-terminal signaling motifs may work synergistically to elicit its effects within B cells. Previous reports provide evidence that the conserved K15 motifs, specifically the PPLP and YEEV motifs, within the K15 C-terminal tail act cooperatively to inhibit BCR signaling (*8*). Hence, it will be relevant to understand whether the other conserved cytoplasmic motifs of K15 play a role in endocytosis. We have also employed LC-MS/MS to analyze B cell proteins that bind the phosphorylated K15 YEEV motif and have identified downstream effectors of the BCR such as phospholipase C γ1 and γ2, phosphatidylinositol 3′-kinase, and BCR downstream signaling protein 1 (BRDG1) (unpublished results). Therefore, it is possible that the signaling motifs within the K15 C-terminal tail act through multiple mechanisms to modify BCR signaling.

Our results emphasize the ability of proteins encoded by viral and bacterial pathogens to connect with the machinery of infected cells by acquiring short peptide motifs that engage the interaction domains of intracellular polypeptides. The fact that K15 interacts with proteins involved with endocytosis strongly argues that it may influence protein trafficking in infected cells. It will be of interest to pursue the mechanisms by which ITSN2 integrates with other K15-associated cellular proteins.

ACKNOWLEDGMENT

The authors thank Dr. Jae U. Jung for the K15 cDNA and Dr. Clark D. Wells, Dr. Karen Colwill, Dr. Claus Jorgensen, and Marilyn Goudreault for invaluable reagents.

REFERENCES

1. Choi, J., Means, R. E., Damania, B., and Jung, J. U. (2001) Molecular piracy of Kaposi's sarcoma associated herpesvirus, *Cytokine Growth Factor Rev. 12*, 245−257.
2. Chang, Y., Cesarman, E., Pessin, M. S., Lee, F., Culpepper, J., Knowles, D. M., and Moore, P. S. (1994) Identification of herpesvirus-like DNA sequences in AIDS-associated Kaposi's sarcoma, *Science 266*, 1865−1869.
3. Schulz, T. F. (2001) KSHV/HHV8-associated lymphoproliferations in the AIDS setting, *Eur. J. Cancer 37*, 1217−1226.
4. Boshoff, C., Schulz, T. F., Kennedy, M. M., Graham, A. K., Fisher, C., Thomas, A., McGee, J. O., Weiss, R. A., and O'Leary, J. J. (1995) Kaposi's sarcoma-associated herpesvirus infects endothelial and spindle cells, *Nat. Med. 1*, 1274−1278.
5. Li, J. J., Huang, Y. Q., Cockerell, C. J., and Friedman-Kien, A. E. (1996) Localization of human herpes-like virus type 8 in vascular endothelial cells and perivascular spindle-shaped cells of Kaposi's sarcoma lesions by in situ hybridization, *Am. J. Pathol. 148*, 1741−1748.
6. Dupin, N., Fisher, C., Kellam, P., Ariad, S., Tulliez, M., Franck, N., van Marck, E., Salmon, D., Gorin, I., Escande, J. P., Weiss,

R. A., Alitalo, K., and Boshoff, C. (1999) Distribution of human herpesvirus-8 latently infected cells in Kaposi's sarcoma, multicentric Castleman's disease, and primary effusion lymphoma, *Proc. Natl. Acad. Sci. U.S.A. 96*, 4546−4551.
7. Jenner, R. G., and Boshoff, C. (2002) The molecular pathology of Kaposi's sarcoma-associated herpesvirus, *Biochim. Biophys. Acta 1602*, 1−22.
8. Choi, J. K., Lee, B. S., Shim, S. N., Li, M., and Jung, J. U. (2000) Identification of the novel K15 gene at the rightmost end of the Kaposi's sarcoma-associated herpesvirus genome, *J. Virol. 74*, 436−46.
9. Poole, L. J., Zong, J. C., Ciufo, D. M., Alcendor, D. J., Cannon, J. S., Ambinder, R., Orenstein, J. M., Reitz, M. S., and Hayward, G. S. (1999) Comparison of genetic variability at multiple loci across the genomes of the major subtypes of Kaposi's sarcoma-associated herpesvirus reveals evidence for recombination and for two distinct types of open reading frame K15 alleles at the right-hand end, *J. Virol. 73*, 6646−6660.
10. Glenn, M., Rainbow, L., Aurade, F., Davison, A., and Schulz, T. F. (1999) Identification of a spliced gene from Kaposi's sarcoma-associated herpesvirus encoding a protein with similarities to latent membrane proteins 1 and 2A of Epstein-Barr virus, *J. Virol. 73*, 6953−63.
11. Burkhardt, A. L., Bolen, J. B., Kieff, E., and Longnecker, R. (1992) An Epstein-Barr virus transformation-associated membrane protein interacts with src family tyrosine kinases, *J. Virol. 66*, 5161−5167.
12. Winberg, G., Matskova, L., Chen, F., Plant, P., Rotin, D., Gish, G., Ingham, R., Ernberg, I., and Pawson, T. (2000) Latent membrane protein 2A of Epstein-Barr virus binds WW domain E3 protein-ubiquitin ligases that ubiquitinate B-cell tyrosine kinases, *Mol. Cell. Biol. 20*, 8526−8535.
13. Brinkmann, M. M., and Schulz, T. F. (2006) Regulation of intracellular signalling by the terminal membrane proteins of members of the Gammaherpesvirinae, *J. Gen. Virol. 87*, 1047−1074.
14. Miller, C. L., Lee, J. H., Kieff, E., and Longnecker, R. (1994) An integral membrane protein (LMP2) blocks reactivation of Epstein-Barr virus from latency following surface immunoglobulin crosslinking, *Proc. Natl. Acad. Sci. U.S.A. 91*, 772−776.
15. Fruehling, S., and Longnecker, R. (1997) The immunoreceptor tyrosine-based activation motif of Epstein-Barr virus LMP2A is essential for blocking BCR-mediated signal transduction, *Virology 235*, 241−251.
16. Miller, C. L., Burkhardt, A. L., Lee, J. H., Stealey, B., Longnecker, R., Bolen, J. B., and Kieff, E. (1995) Integral membrane protein 2 of Epstein-Barr virus regulates reactivation from latency through dominant negative effects on protein-tyrosine kinases, *Immunity 2*, 155−166.
17. Jenner, R. G., Alba, M. M., Boshoff, C., and Kellam, P. (2001) Kaposi's sarcoma-associated herpesvirus latent and lytic gene expression as revealed by DNA arrays, *J. Virol. 75*, 891−902.
18. Wong, E. L., and Damania, B. (2006) Transcriptional regulation of the Kaposi's sarcoma-associated herpesvirus K15 gene, *J. Virol. 80*, 1385−1392.
19. Paulose-Murphy, M., Ha, N. K., Xiang, C., Chen, Y., Gillim, L., Yarchoan, R., Meltzer, P., Bittner, M., Trent, J., and Zeichner, S. (2001) Transcription program of human herpesvirus 8 (Kaposi's sarcoma-associated herpesvirus), *J. Virol. 75*, 4843−4853.
20. Brinkmann, M. M., Glenn, M., Rainbow, L., Kieser, A., Henke-Gendo, C., and Schulz, T. F. (2003) Activation of mitogen-activated protein kinase and NF-kappaB pathways by a Kaposi's sarcoma-associated herpesvirus K15 membrane protein, *J. Virol. 77*, 9346−9358.
21. Sharp, T. V., Wang, H. W., Koumi, A., Hollyman, D., Endo, Y., Ye, H., Du, M. Q., and Boshoff, C. (2002) K15 protein of Kaposi's sarcoma-associated herpesvirus is latently expressed and binds to HAX-1, a protein with antiapoptotic function, *J. Virol. 76*, 802−816.
22. Colwill, K., Wells, C. D., Elder, K., Goudreault, M., Hersi, K., Kulkarni, S., Hardy, W. R., Pawson, T., and Morin, G. B. (2006) Modification of the Creator recombination system for proteomics applications—improved expression by addition of splice sites, *BMC Biotechnol. 6*, 13.
23. Ingham, R. J., Colwill, K., Howard, C., Dettwiler, S., Lim, C. S., Yu, J., Hersi, K., Raaijmakers, J., Gish, G., Mbamalu, G., Taylor, L., Yeung, B., Vassilovski, G., Amin, M., Chen, F., Matskova, L., Winberg, G., Ernberg, I., Linding, R., O'Donnell, P., Starostine, A., Keller, W., Metalnikov, P., Stark, C., and Pawson, T. (2005) WW domains provide a platform for the assembly of multiprotein networks, *Mol. Cell. Biol. 25*, 7092−7106.
24. Rich, R. L., and Myszka, D. G. (2000) Advances in surface plasmon resonance biosensor analysis, *Curr. Opin. Biotechnol. 11*, 54−61.
25. Plant, P. J., Fawcett, J. P., Lin, D. C., Holdorf, A. D., Binns, K., Kulkarni, S., and Pawson, T. (2003) A polarity complex of mPar-6 and atypical PKC binds, phosphorylates and regulates mammalian Lgl, *Nat. Cell Biol. 5*, 301−308.
26. Pucharcos, C., Estivill, X., and de la Luna, S. (2000) Intersectin 2, a new multimodular protein involved in clathrin-mediated endocytosis, *FEBS Lett. 478*, 43−51.
27. Coda, L., Salcini, A. E., Confalonieri, S., Pelicci, G., Sorkina, T., Sorkin, A., Pelicci, P. G., and Di Fiore, P. P. (1998) Eps15R is a tyrosine kinase substrate with characteristics of a docking protein possibly involved in coated pits-mediated internalization, *J. Biol. Chem. 273*, 3003−3012.
28. Modregger, J., Ritter, B., Witter, B., Paulsson, M., and Plomann, M. (2000) All three PACSIN isoforms bind to endocytic proteins and inhibit endocytosis, *J. Cell Sci. 113* (Part 24), 4511−4521.
29. Marsh, M., and McMahon, H. T. (1999) The structural era of endocytosis, *Science 285*, 215−220.
30. O'Bryan, J. P., Mohney, R. P., and Oldham, C. E. (2001) Mitogenesis and endocytosis: What's at the INTERSECTIoN?, *Oncogene 20*, 6300−6308.
31. Qualmann, B., Roos, J., DiGregorio, P. J., and Kelly, R. B. (1999) Syndapin I, a synaptic dynamin-binding protein that associates with the neural Wiskott-Aldrich syndrome protein, *Mol. Biol. Cell 10*, 501−513.
32. Sengar, A. S., Wang, W., Bishay, J., Cohen, S., and Egan, S. E. (1999) The EH and SH3 domain Ese proteins regulate endocytosis by linking to dynamin and Eps15, *EMBO J. 18*, 1159−1171.
33. Seet, B. T., Berry, D. M., Maltzman, J. S., Shabason, J., Raina, M., Koretzky, G. A., McGlade, C. J., and Pawson, T. (2007) Efficient T-cell receptor signaling requires a high-affinity interaction between the Gads C-SH3 domain and the SLP-76 RxxK motif, *EMBO J. 26*, 678−689.
34. Nguyen, J. T., Turck, C. W., Cohen, F. E., Zuckermann, R. N., and Lim, W. A. (1998) Exploiting the basis of proline recognition by SH3 and WW domains: design of N-substituted inhibitors, *Science 282*, 2088−2092.
35. Zarrinpar, A., Bhattacharyya, R. P., and Lim, W. A. (2003) The structure and function of proline recognition domains, *Sci. STKE 2003*, RE8.
36. Simpson, F., Hussain, N. K., Qualmann, B., Kelly, R. B., Kay, B. K., McPherson, P. S., and Schmid, S. L. (1999) SH3-domain-containing proteins function at distinct steps in clathrin-coated vesicle formation, *Nat. Cell Biol. 1*, 119−124.
37. Ingham, R. J., Raaijmakers, J., Lim, C. S., Mbamalu, G., Gish, G., Chen, F., Matskova, L., Ernberg, I., Winberg, G., and Pawson, T. (2005) The Epstein-Barr virus protein, latent membrane protein 2A, co-opts tyrosine kinases used by the T cell receptor, *J. Biol. Chem. 280*, 34133−34142.
38. Hussain, N. K., Yamabhai, M., Ramjaun, A. R., Guy, A. M., Baranes, D., O'Bryan, J. P., Der, C. J., Kay, B. K., and McPherson, P. S. (1999) Splice variants of intersectin are components of the endocytic machinery in neurons and nonneuronal cells. *J. Biol. Chem. 274*, 15671−15677.
39. Di, Fiore, P. P., Pelicci, P. G., and Sorkin, A. (1997) EH: a novel protein-protein interaction domain potentially involved in intracellular sorting, *Trends Biochem. Sci. 22*, 411−413.
40. Okamoto, M., Schoch, S., and Sudhof, T. C. (1999) EHSH1/intersectin, a protein that contains EH and SH3 domains and binds to dynamin and SNAP-25. A protein connection between exocytosis and endocytosis?, *J. Biol. Chem. 274*, 18446−18454.
41. Tong, X. K., Hussain, N. K., de Heuvel, E., Kurakin, A., Abi-Jaoude, E., Quinn, C. C., Olson, M. F., Marais, R., Baranes, D., Kay, B. K., and McPherson, P. S. (2000) The endocytic protein intersectin is a major binding partner for the Ras exchange factor mSos1 in rat brain, *EMBO J. 19*, 1263−1271.
42. McGavin, M. K., Badour, K., Hardy, L. A., Kubiseski, T. J., Zhang, J., and Siminovitch, K. A. (2001) The intersectin 2 adaptor links Wiskott Aldrich syndrome protein (WASp)-mediated actin polymerization to T cell antigen receptor endocytosis, *J. Exp. Med. 194*, 1777−1787.
43. Sparks, A. B., Rider, J. E., and Kay, B. K. (1998) Mapping the specificity of SH3 domains with phage-displayed random-peptide libraries, *Methods Mol. Biol. 84*, 87−103.

44. Sparks, A. B., Rider, J. E., Hoffman, N. G., Fowlkes, D. M., Quillam, L. A., and Kay, B. K. (1996) Distinct ligand preferences of Src homology 3 domains from Src, Yes, Abl, Cortactin, p53bp2, PLCgamma, Crk, and Grb2, *Proc. Natl. Acad. Sci. U.S.A. 93*, 1540−1544.

45. Garrus, J. E., von Schwedler, U. K., Pornillos, O. W., Morham, S. G., Zavitz, K. H., Wang, H. E., Wettstein, D. A., Stray, K. M., Cote, M., Rich, R. L., Myszka, D. G., and Sundquist, W. I. (2001) Tsg101 and the vacuolar protein sorting pathway are essential for HIV-1 budding, *Cell 107*, 55−65.

46. von Schwedler, U. K., Stuchell, M., Muller, B., Ward, D. M., Chung, H. Y., Morita, E., Wang, H. E., Davis, T., He, G. P., Cimbora, D. M., Scott, A., Krausslich, H. G., Kaplan, J., Morham, S. G., and Sundquist, W. I. (2003) The protein network of HIV budding, *Cell 114*, 701−713.

47. Lorenzo, M. E., Jung, J. U., and Ploegh, H. L. (2002) Kaposi's sarcoma-associated herpesvirus K3 utilizes the ubiquitin-proteasome system in routing class major histocompatibility complexes to late endocytic compartments, *J. Virol. 76*, 5522−5531.

BI700357S